Room temperature intraband photodetection at 1.3-1.5 μm in self assembled GaN/AlN quantum dots

A. Vardi, G. Bahir

Department of Electrical Engineering

Technion-Israel Institute of Technology,

Haifa, Israel

M. Tchernycheva, L. Doyennette, L. Nevou, and F. H. Julien

Institut d'Electronique Fondamentale,

Universite Paris-Sud,

Orsay, France.

F. Guillot and E. Monroy

Equipe mixte CEA-CNRS-UJF

Nanophysique et Semiconducteurs,

Grenoble, France.

Outline

- Motivation
- Introduction
- Sample Growth
- Spectroscopy
- Devices
- Summary

Motivation

- The wide band-gap and the large band-offsets of the III-nitride system offers prospects for tunable intraband devices operating at telecommunication wavelengths at room temperature.

Bandgap difference ~ 2.7eV

Lattice mismatch ~2.4%

Very fast relaxation time

in the range 100-200 fs

Future applications: QCL, Modulators, QDIPs

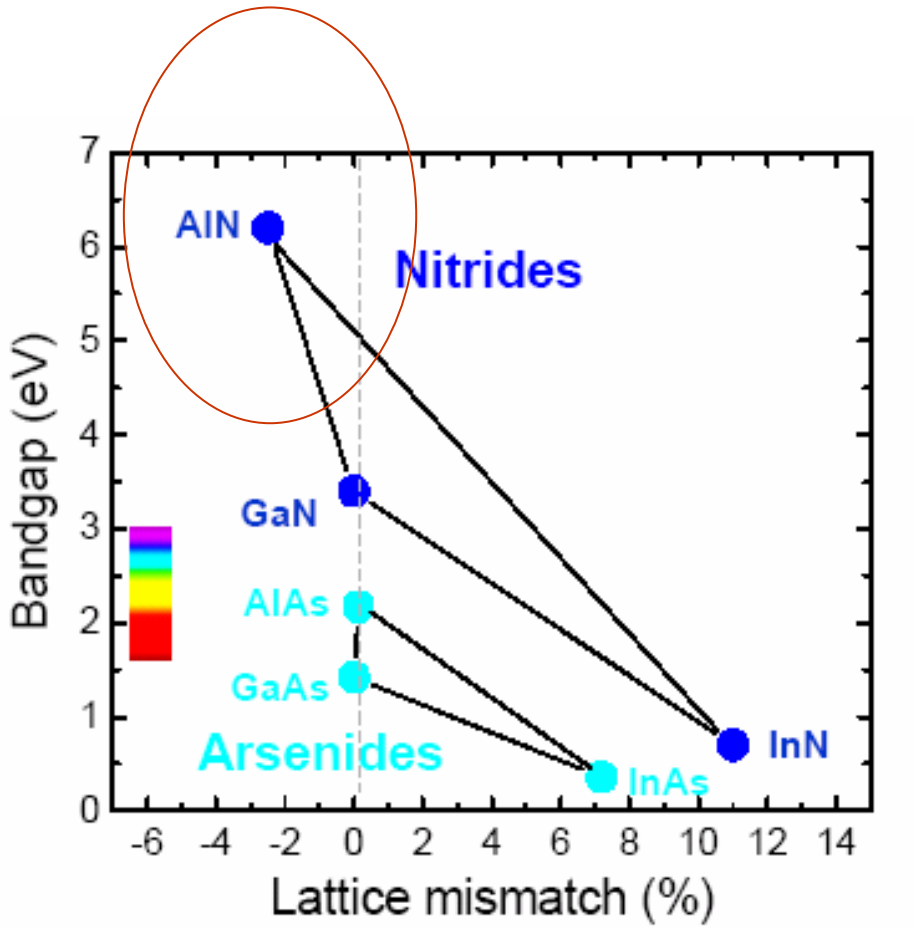

Polarization fields

Spontaneous Polarization

$P_{sp,z}$

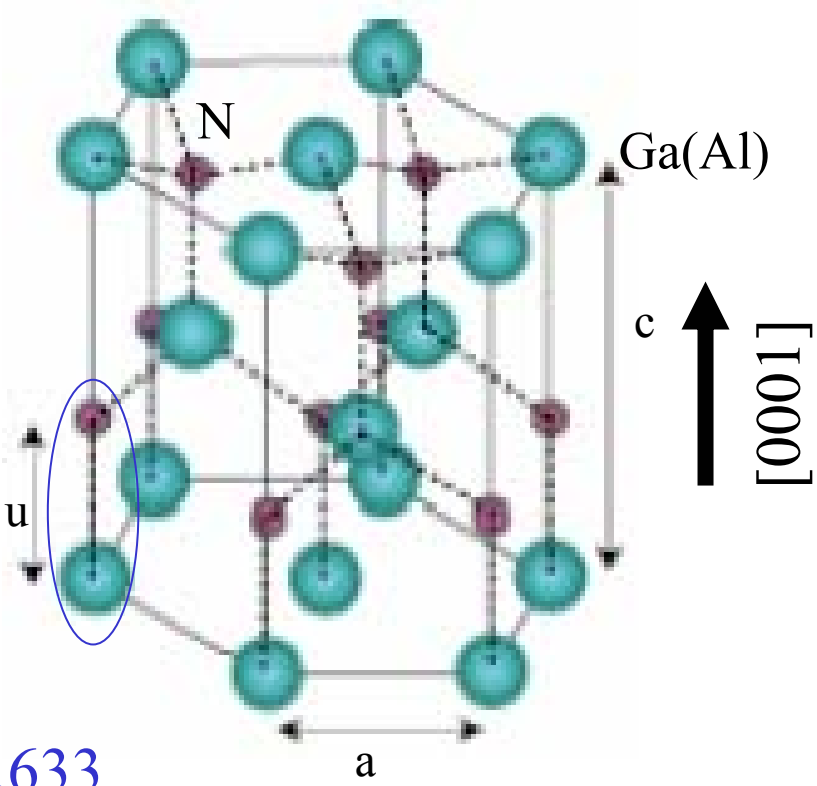

Hexagonal Phase

Wurtzite

Ideal: u/c=0.375, c/a=1.633
GaN: u/c=0.376, c/a=1.627
AlN: u/c=0.38, c/a=1.601

$P_{sp,z}(GaN)=-0.029 C/m^2$
$P_{sp,z}(AlN)=-0.081 C/m2$

F. Bernadini et al, PRB 56, 10024 (1997)

Polarization fields

$$\begin{pmatrix} P_{pz,x} \\ P_{pz,y} \\ P_{pz,z} \end{pmatrix} = \begin{pmatrix} 0 & 0 & 0 & 0 & e_{15} & 0 \\ 0 & 0 & 0 & e_{15} & 0 & 0 \\ e_{31} & e_{31} & e_{33} & 0 & 0 & 0 \end{pmatrix} \begin{pmatrix} \in_{xx} \\ \in_{yy} \\ \in_{zz} \\ \in_{yz} \\ \in_{zx} \\ \in_{xy} \end{pmatrix}$$

Strained GaN on AlN

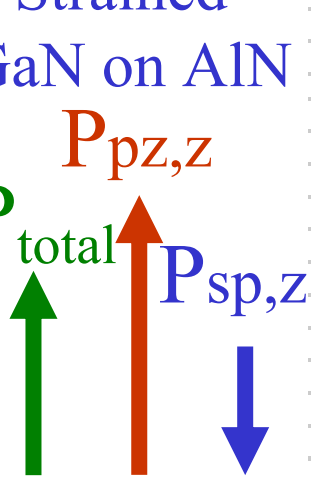

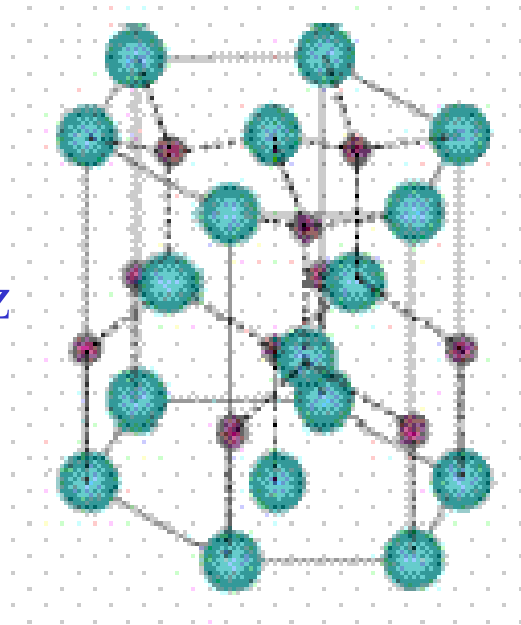

In case of pseudomorphic biaxial strain

$$P_{pz} = P_{pz,z} = e_{33} \in_{zz} + e_{31}(\in_{xx} + \in_{yy})$$

The internal field E is found by solving: $\vec{\nabla} \cdot \vec{D} = 0$

where: $\vec{D} = \varepsilon \vec{E} + \vec{P}, \quad \vec{P} = \vec{P}_{pz} + \vec{P}_{sp}$

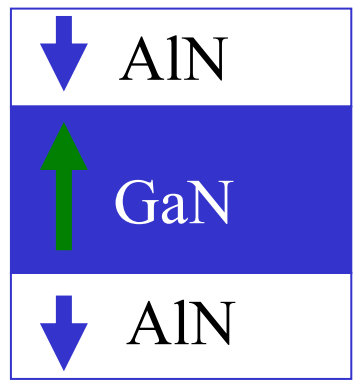

AlN/GaN Heterostructure

Band alignment

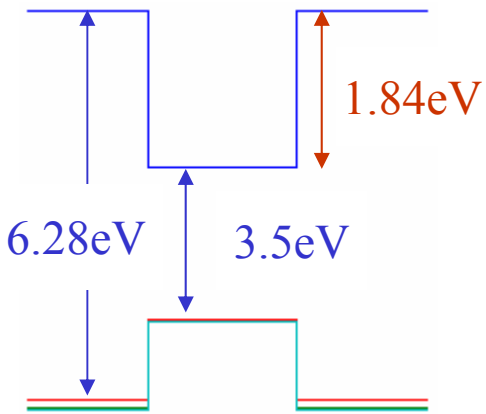

Strain effects

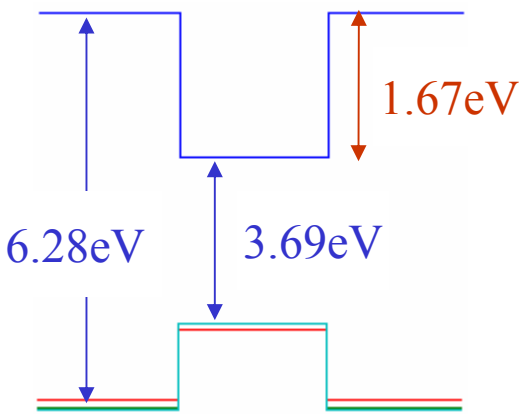

Polarization effects

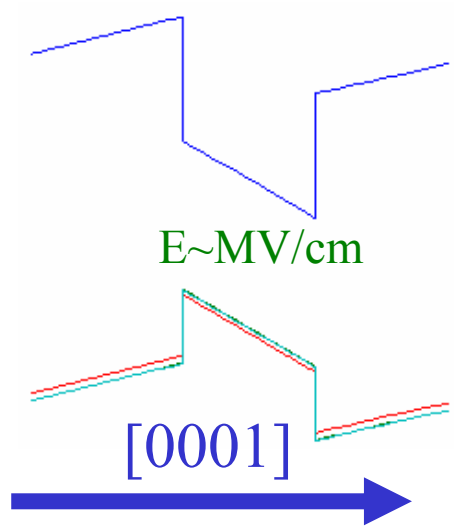

Growth along [0001] axis will emphasize the interplay between the polarization effects and the quantum confinement effects

Samples Growth

Stranski Krastanow (SK) growth mode.

Self assembled QD, 2-3ML wetting layer (WL).

Mono layer (ML)=2.5[A°].

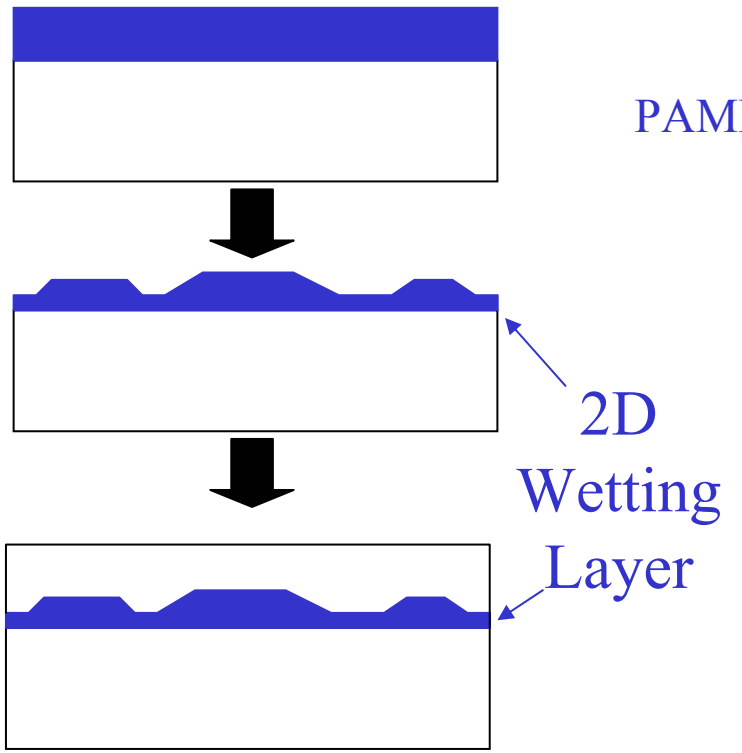

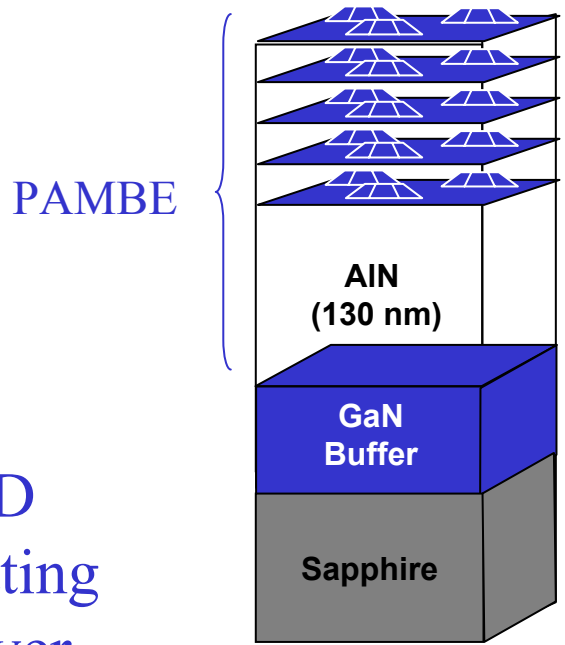

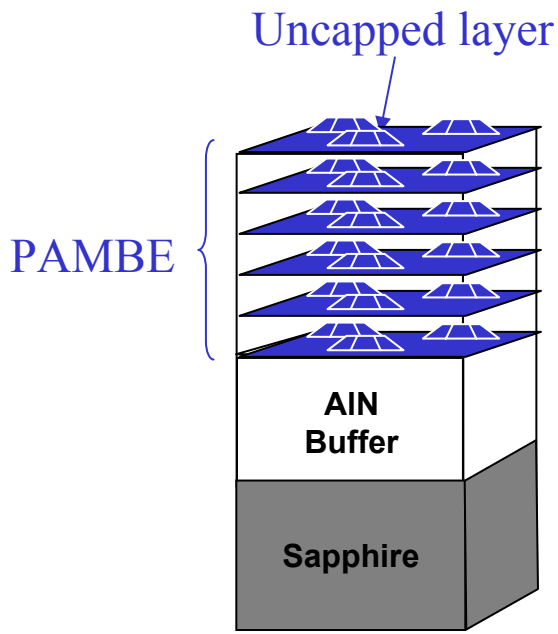

Dot Morphology

The dots have the shape of hexagonal truncated pyramid with {1$\bar{1}$03} facets.

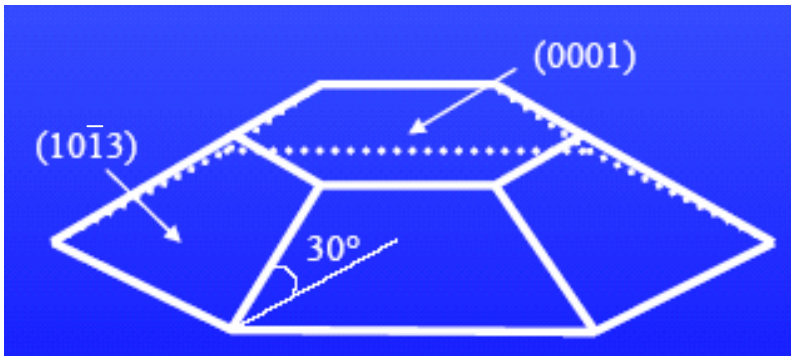

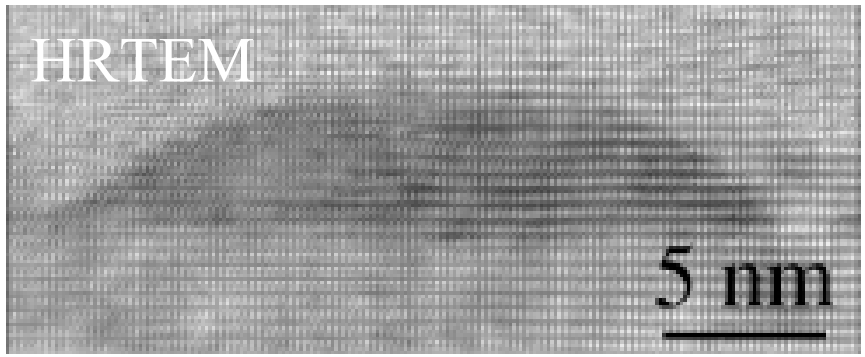

V. Chamard et al, PRB 69,125327(2004)

TEM Characterization

Big Dots

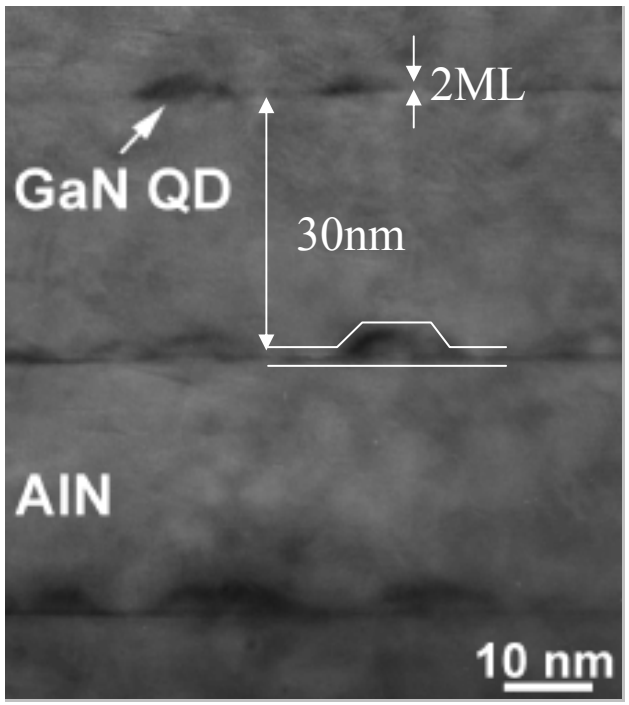

Dot height: 4±1nm

Base diameter: 15±5nm

Small Dots

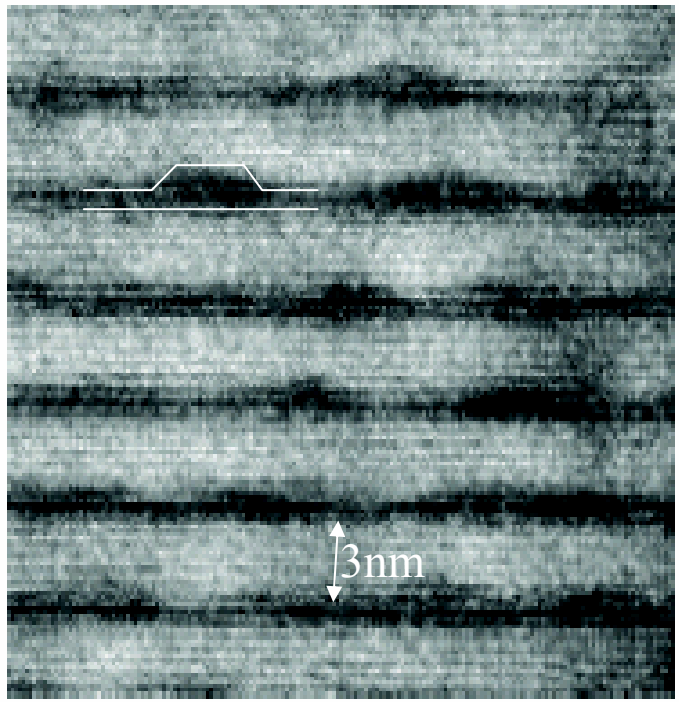

Dot height: 2±1nm

Base diameter: 15±10nm

AFM Characterization

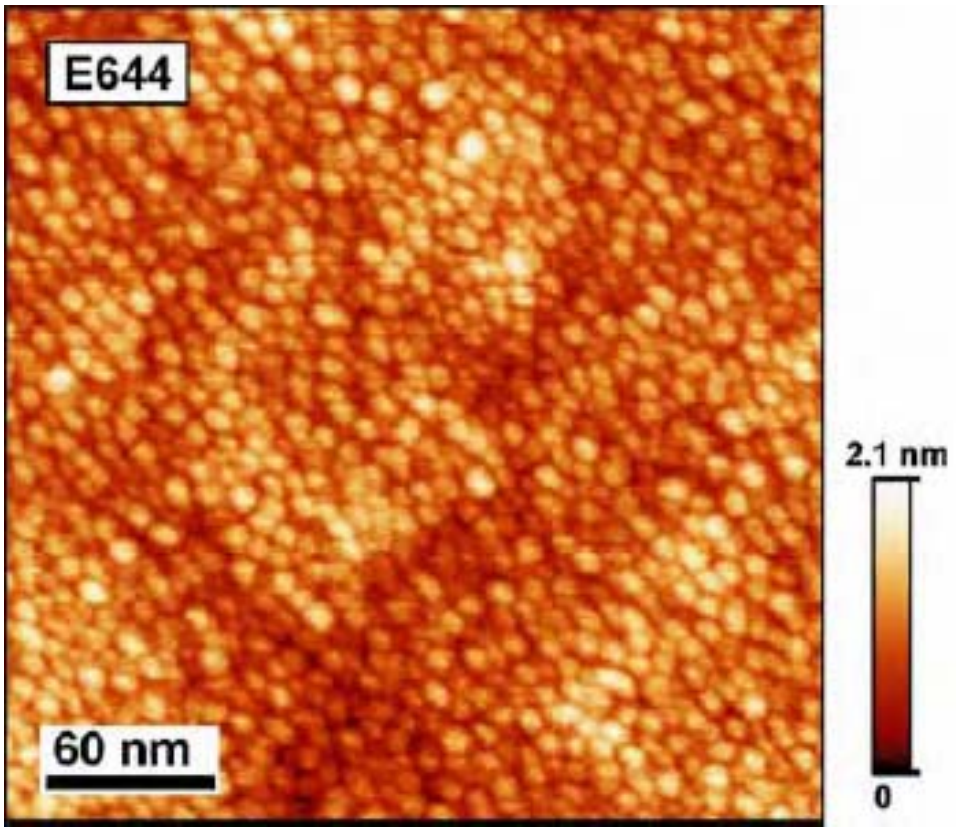

small dots, density:$10^{12}cm^{-2}$

The areal density of the dots is in the range of

10^{11}-$10^{12}cm^{-2}$

for all of the samples

PL Characterization

Big Dots

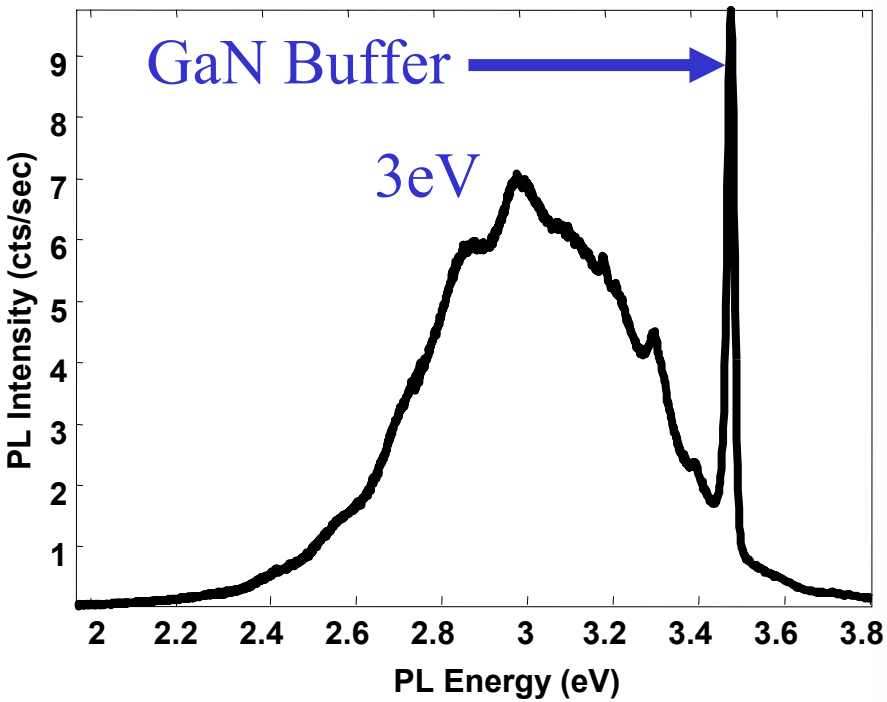

GaN on Sapphire substrate

Small Dots

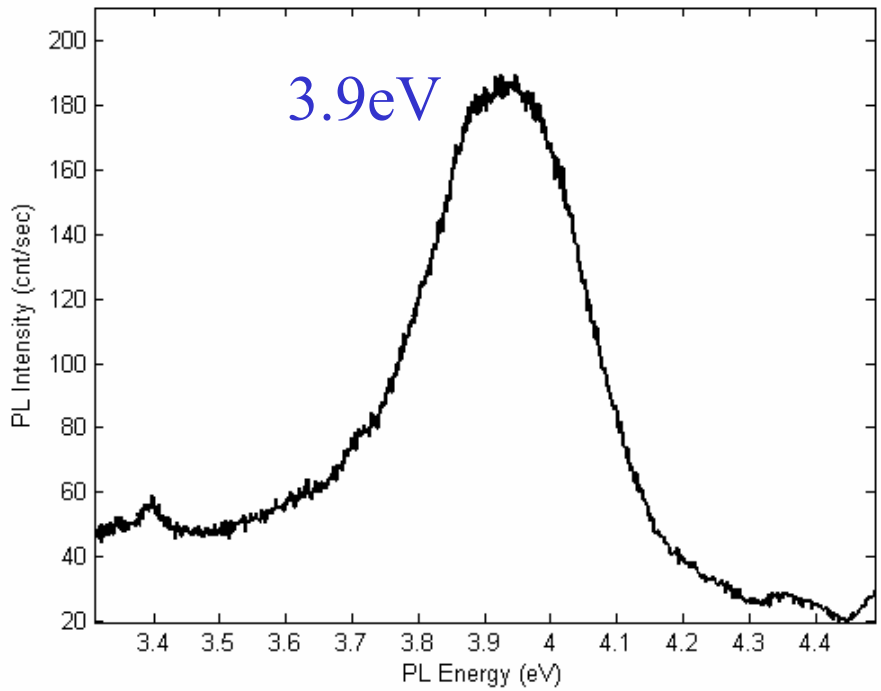

AlN on Sapphire substrate

Measured at 12K, using xenon lamp's light, dispersed by 0.275m monochromator. Excitation wavelength: 251nm.

Evaluation of the Internal Field

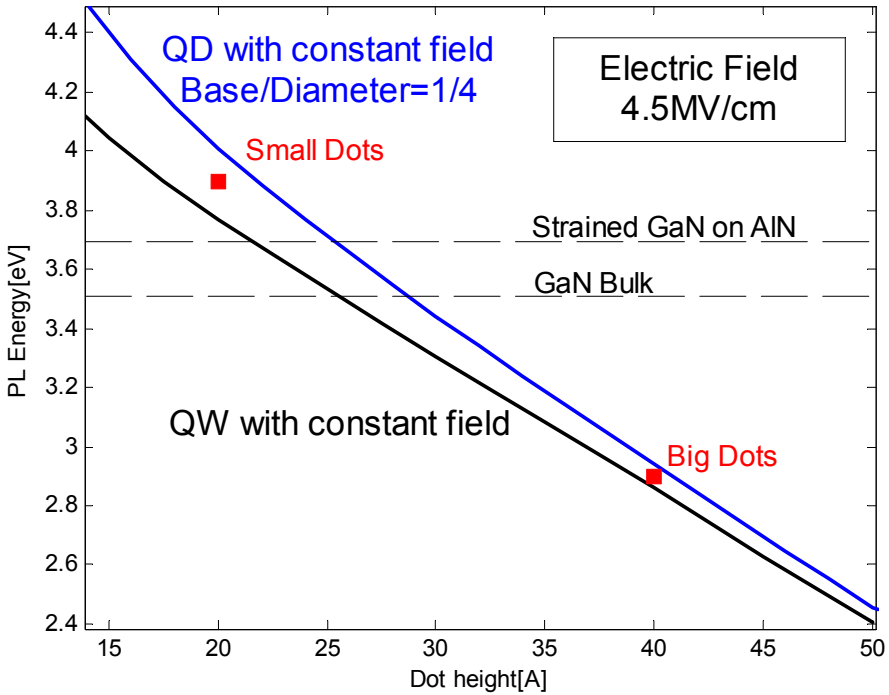

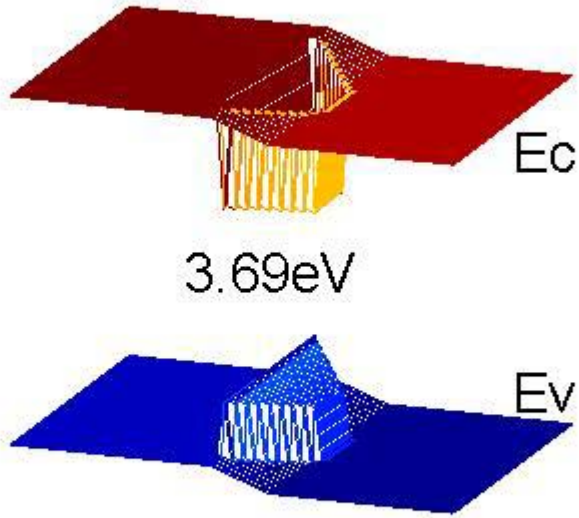

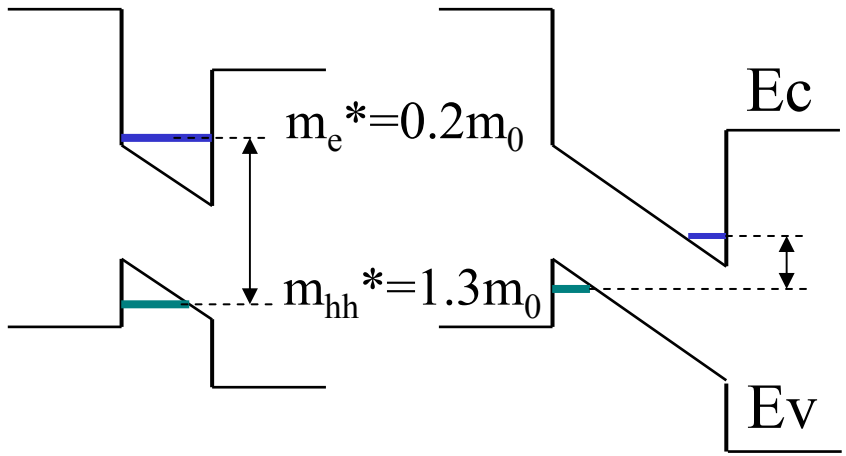

Small dot Big dot

Intraband Transitions

Transitions between states with different parity along the polarization axis (of the light) are preferred.

Growth direction transition

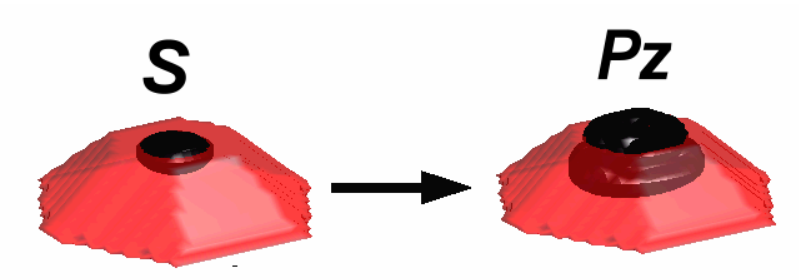

In-plane transitions

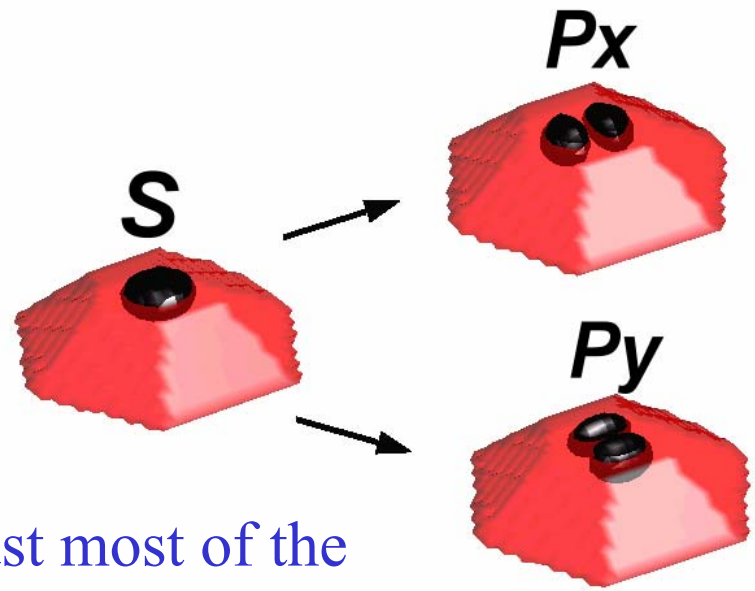

These transitions exhaust most of the ground state - Oscillator strength

Vasanelli et al, Phys. E **11** pg. 41 (2001)

Nextnano simulation

Effective-mass solution in 3D, including strain and polarization effects

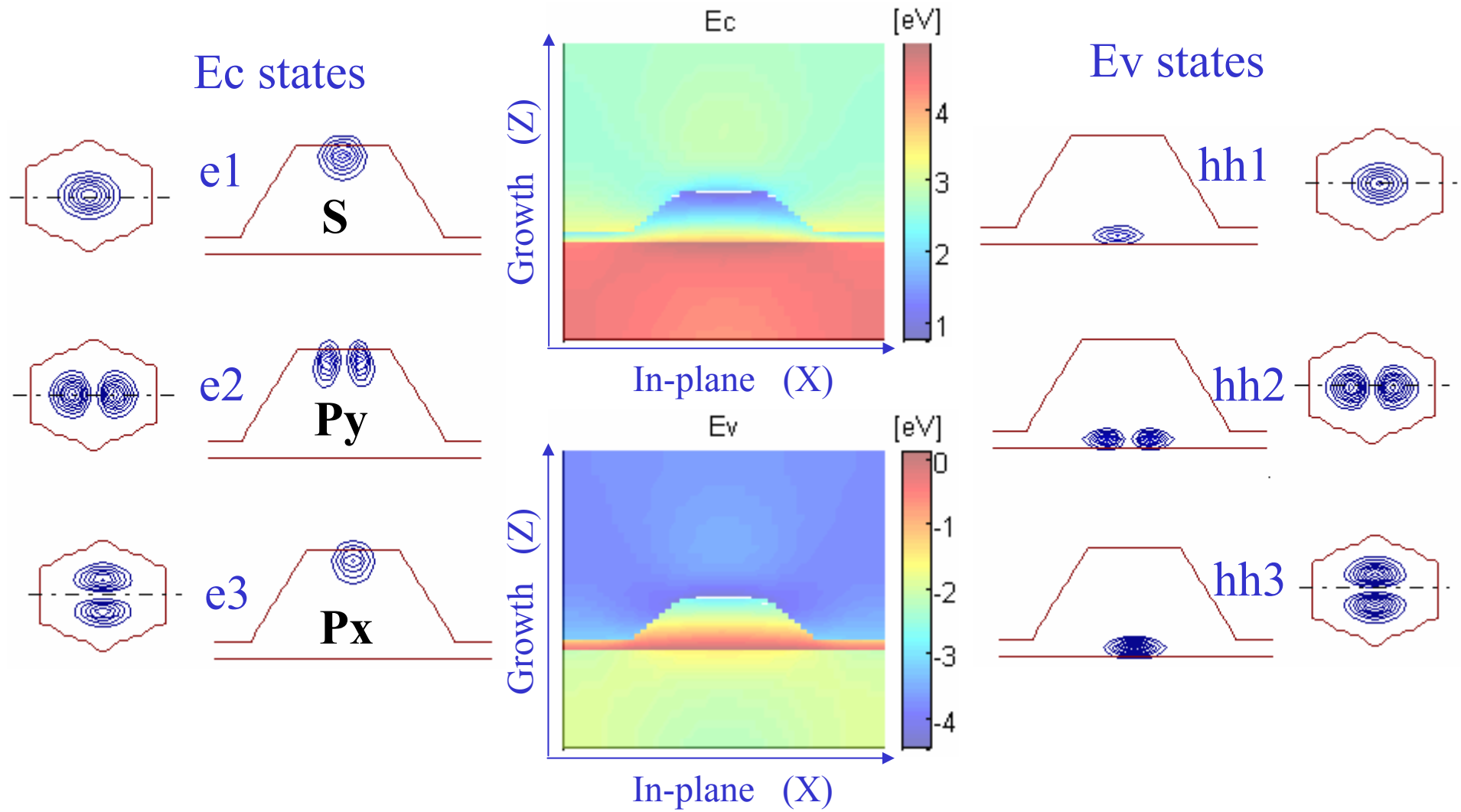

polarization
x pol
y pol
z pol

Nextnano Simulation

Effective-mass solution in 3D, including strain and polarization effects

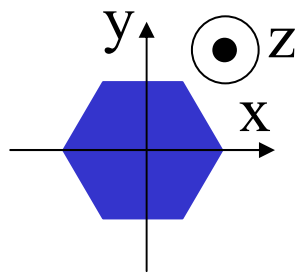

Big Dot

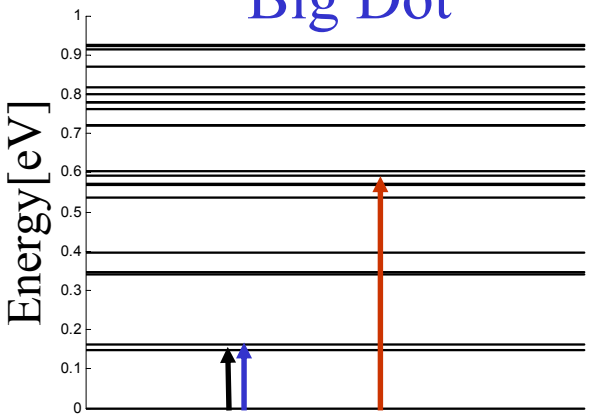

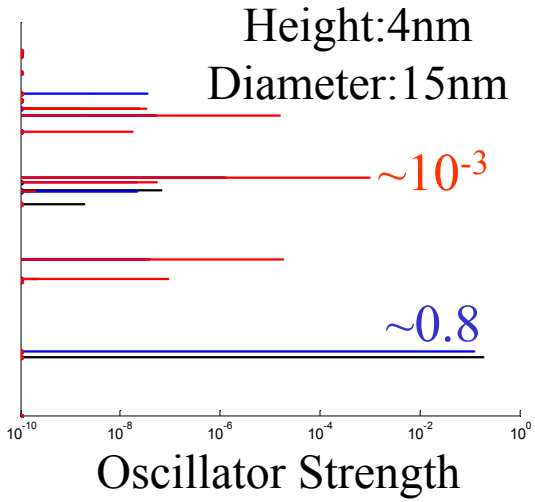

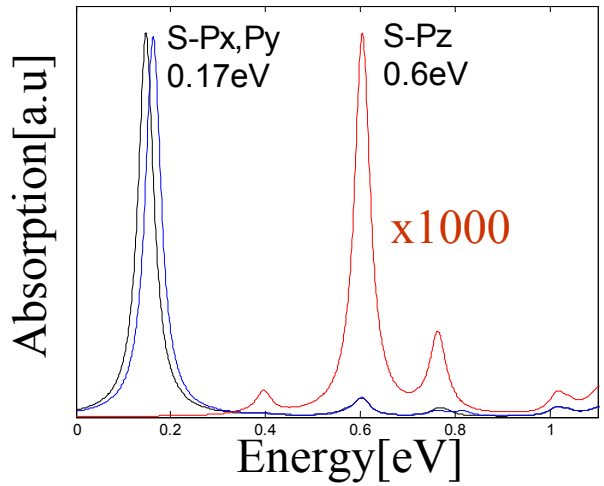

Small Dot

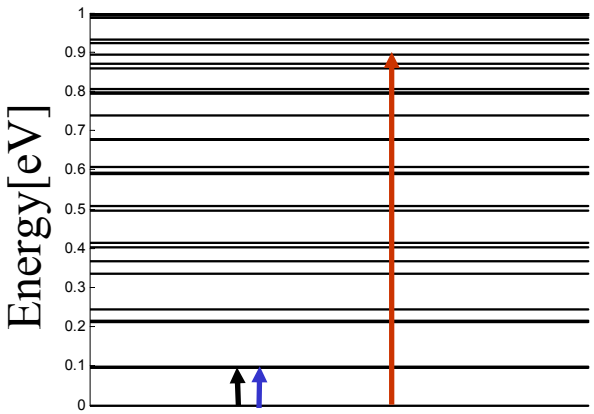

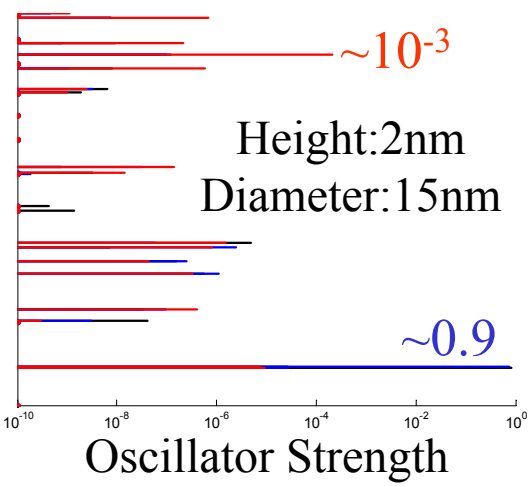

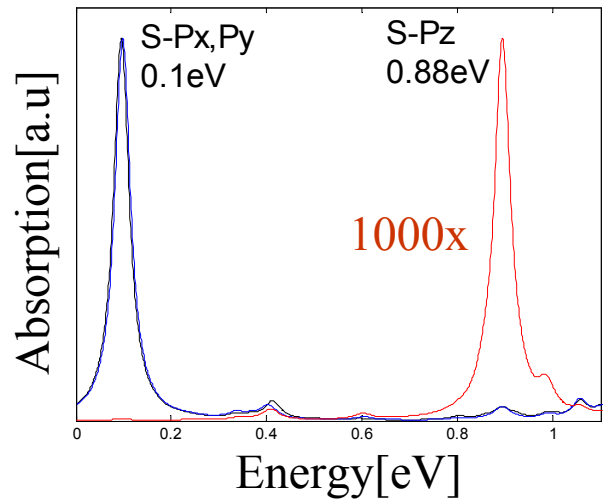

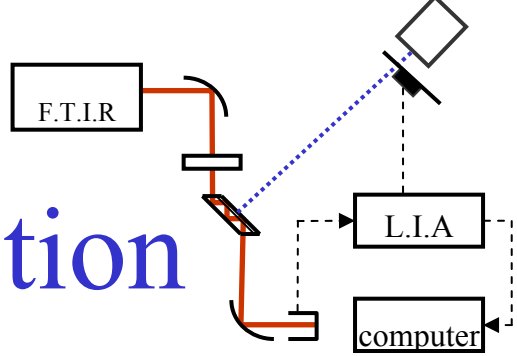

Photo-induced Absorption

Undoped GaN QD, AlN on Sapphire substrate

TM Polarized light

S to Pz transition

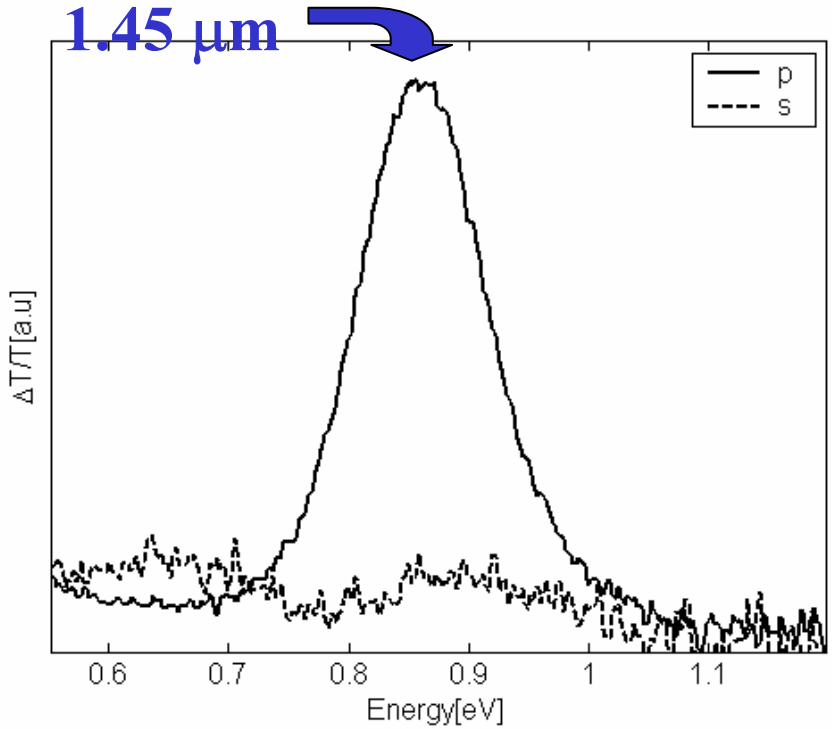

Measured at room temperature, using frequency doubled Argon Laser (244nm), pump power 200mW.

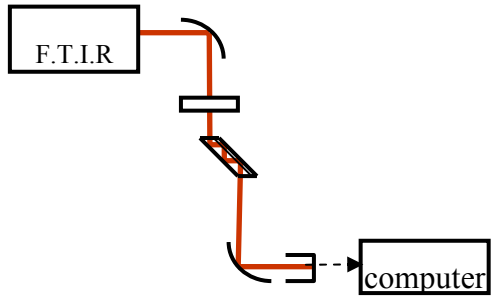

Doped QD

20x GaN QD and 3nm AlN spacers

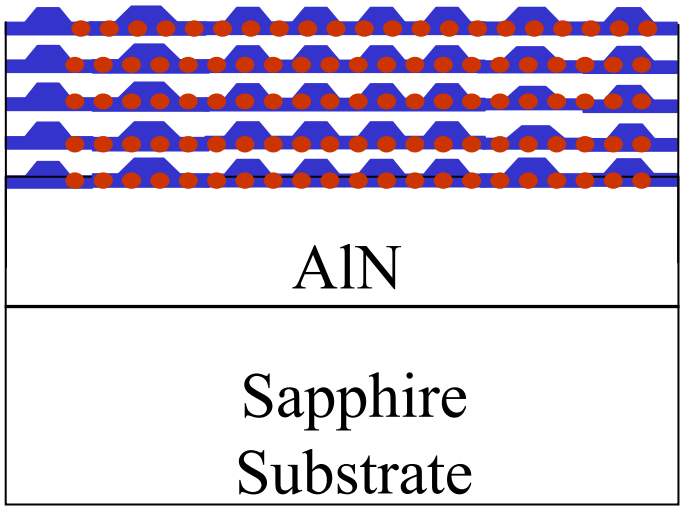

Transmittance

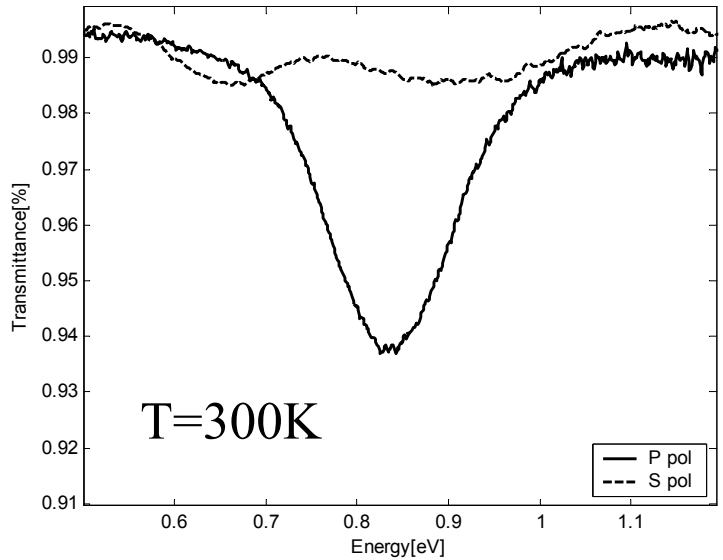

The dots exhibit absorption in the range of 1-2% per reflection which corresponds to $\alpha \sim 10^3 cm^{-1}$.

$$f_{PzS} \sim 10^{-3} \rightarrow \alpha_{PzS} = \frac{\pi \hbar N_d n_{op} e^2}{m^* \varepsilon \varepsilon_0 c} \frac{\Gamma}{\left(\hbar\omega - \hbar\omega_{PzS}\right)^2 + \Gamma^2} \left(N_s - n_{Pz}\right) f_{PzS}$$

one electron per dot

Vertical Device

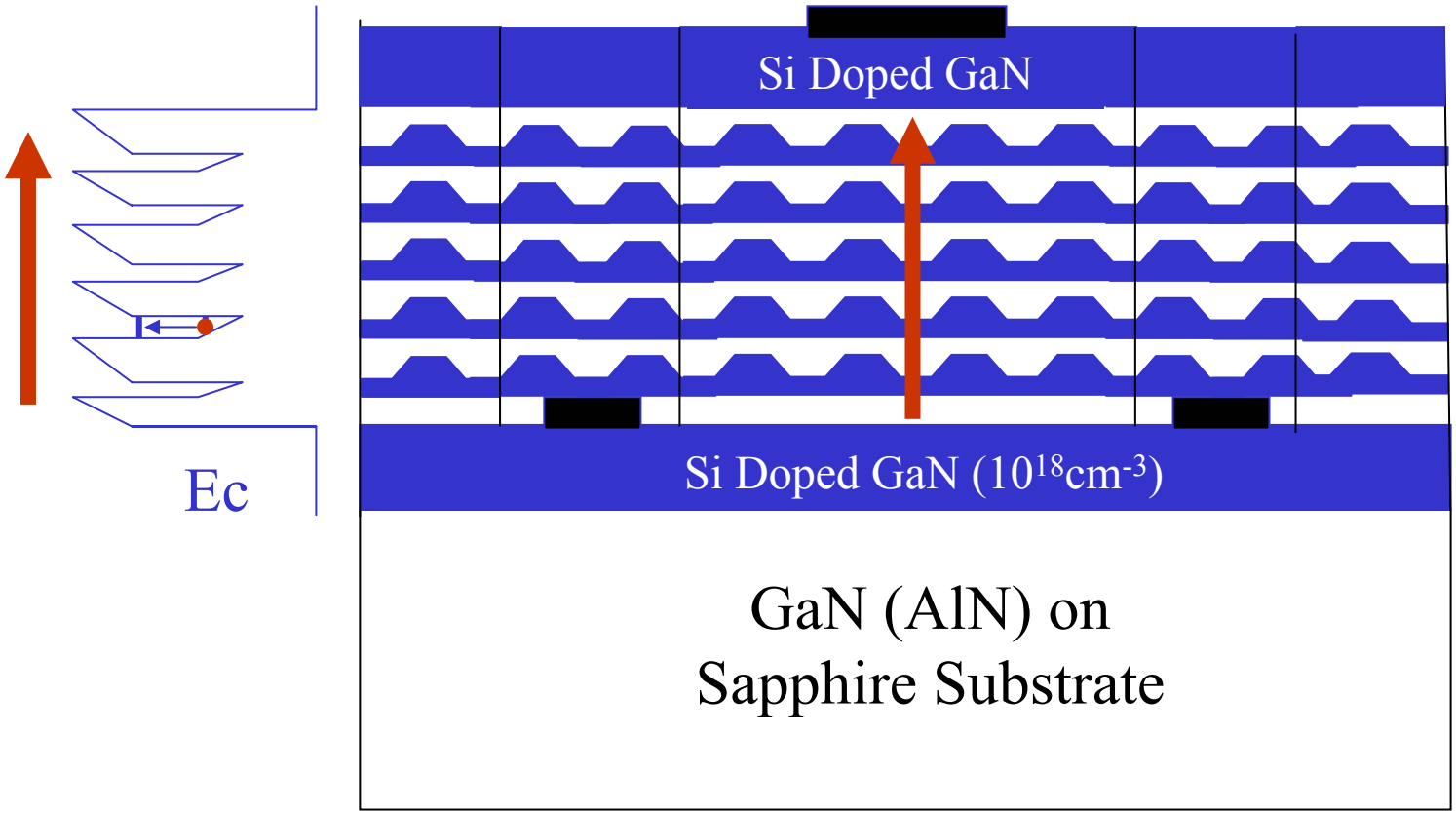

Lateral Device

Interdigitated structure, 10 fingers: 800 μm long, 10 μm spacing

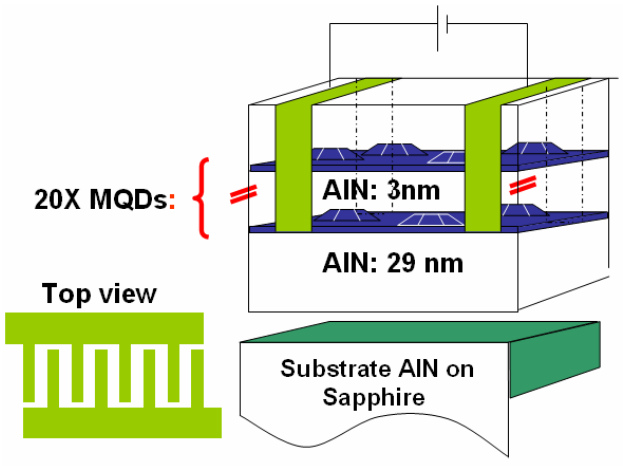

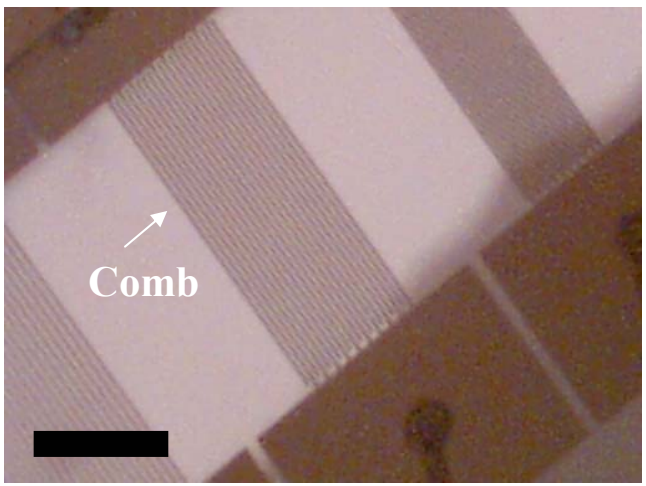

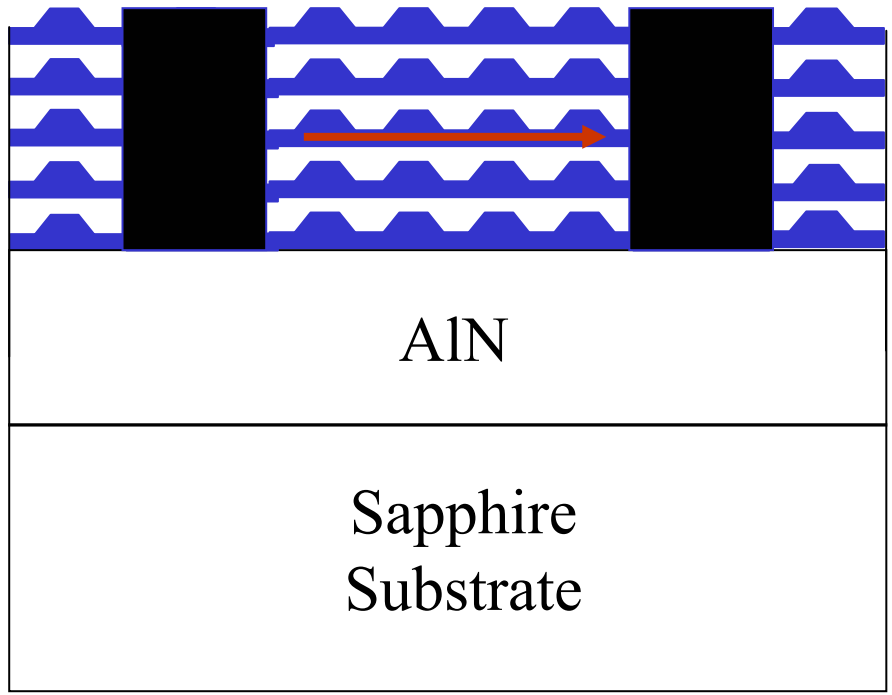

PC Lateral Device

Near IR (NIR) Photocurrent

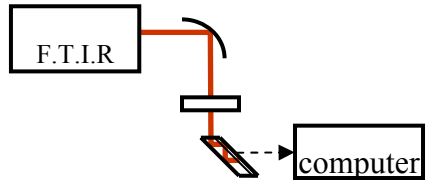

Contacts I-V curve

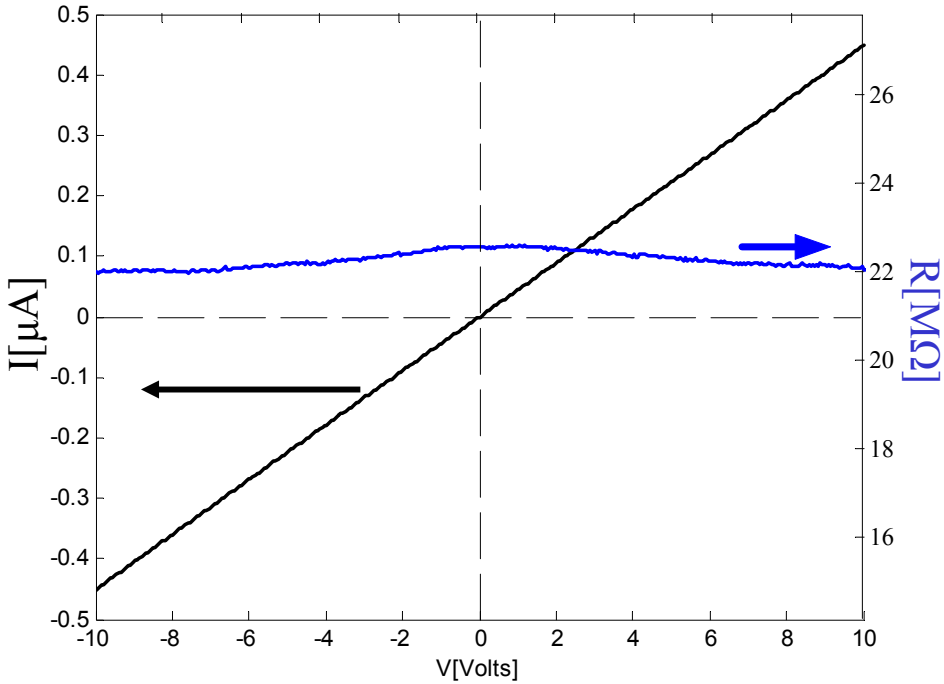

Spectral response

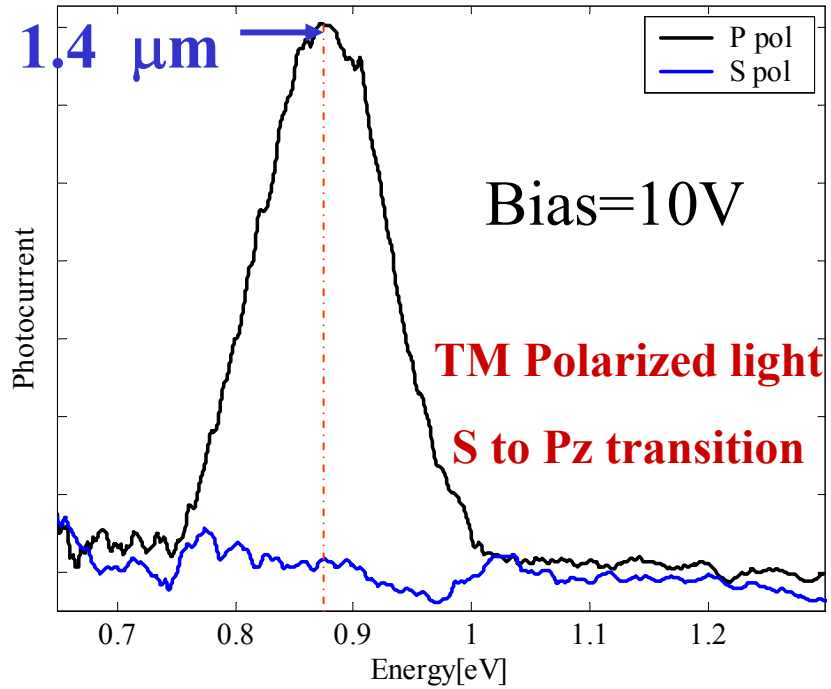

Measured at Room Temperature, Using FTIR with Tungsten-Halogen source.

Submitted to APL

PC Lateral Device

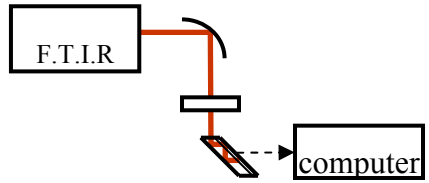

Near IR (NIR) Photocurrent

I-V curve

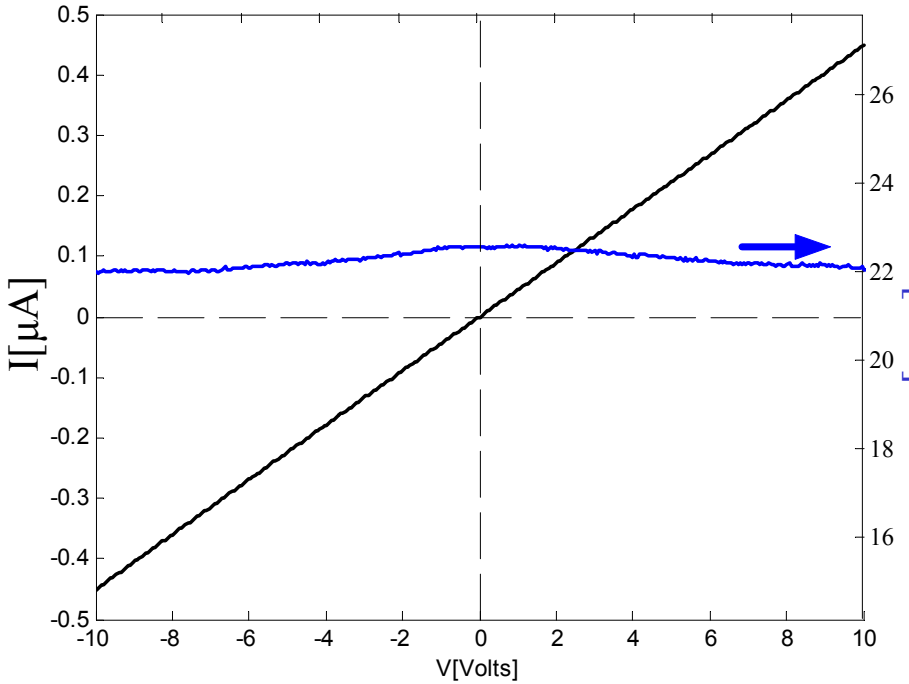

Responsivity

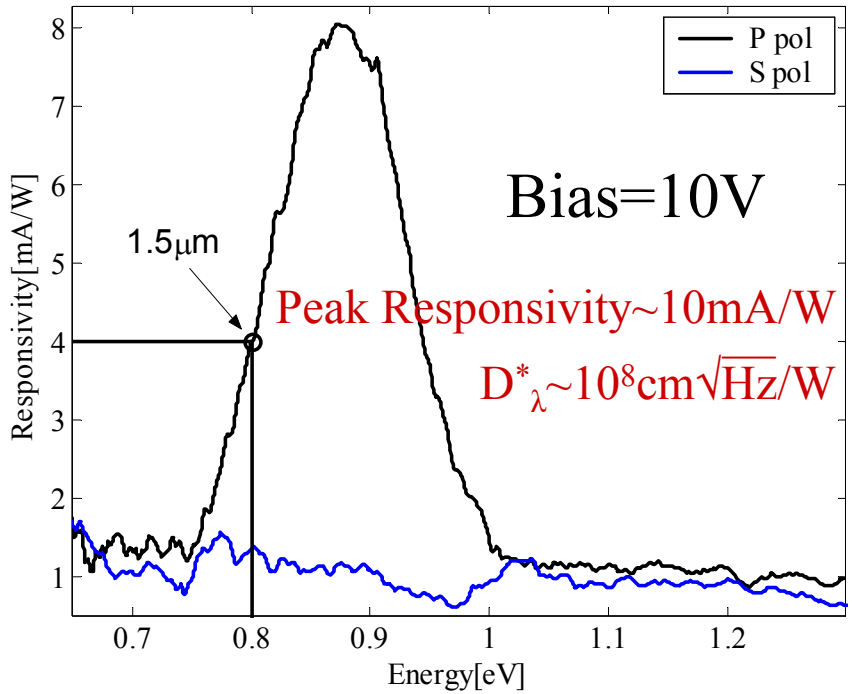

Measured at Room Temperature, Using FTIR with Tungsten-Halogen source.

Vardi APL 2006

PL Vs Intraband Absorption and Photocurrent in Lateral Device

Big Dots → Small Dots

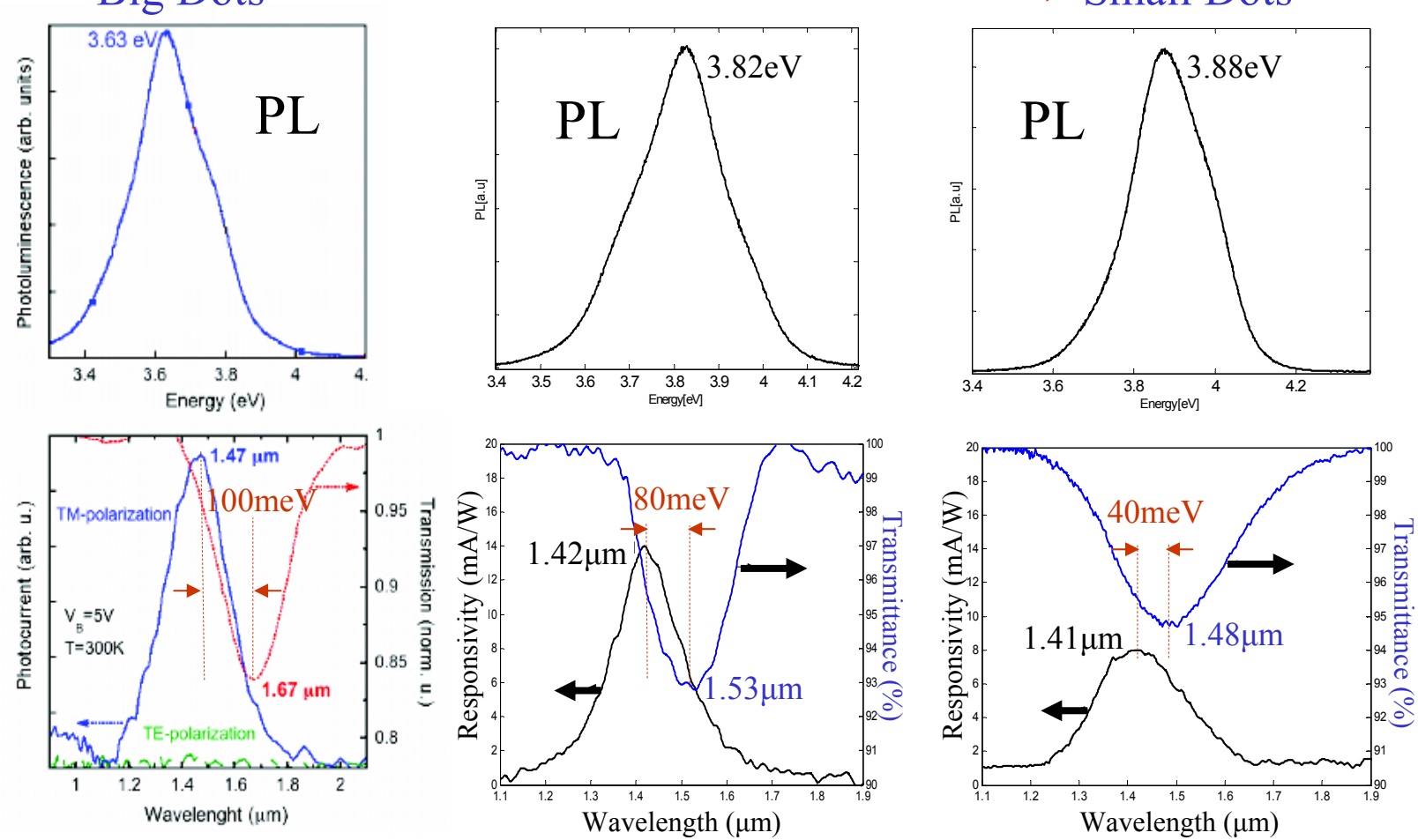

The smaller the dots, the smaller the blue shift.

Lateral Device

Temperature dependence

Absorbance

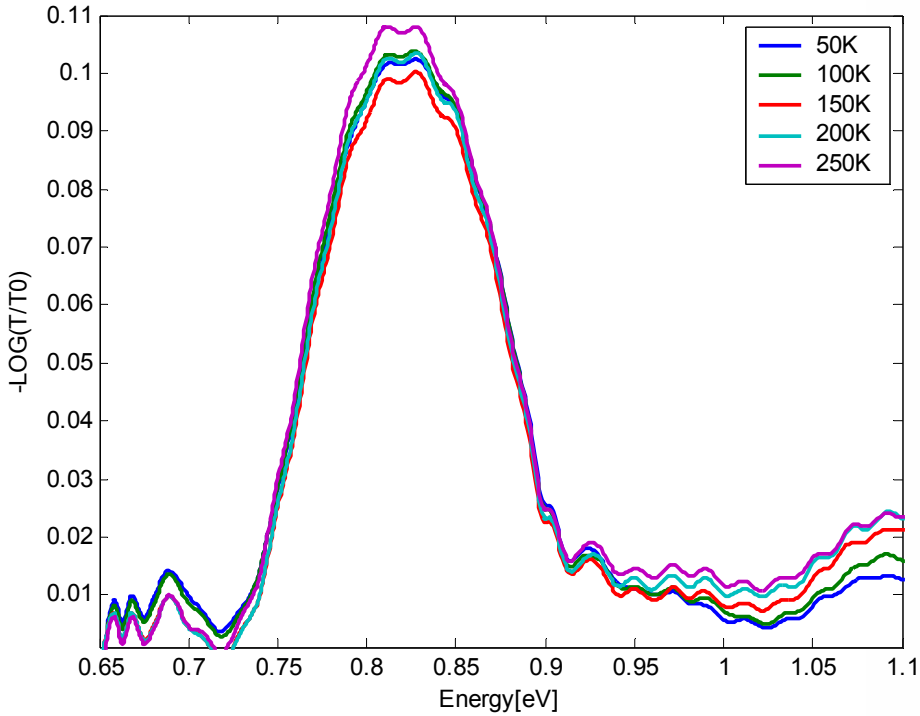

Photocurrent

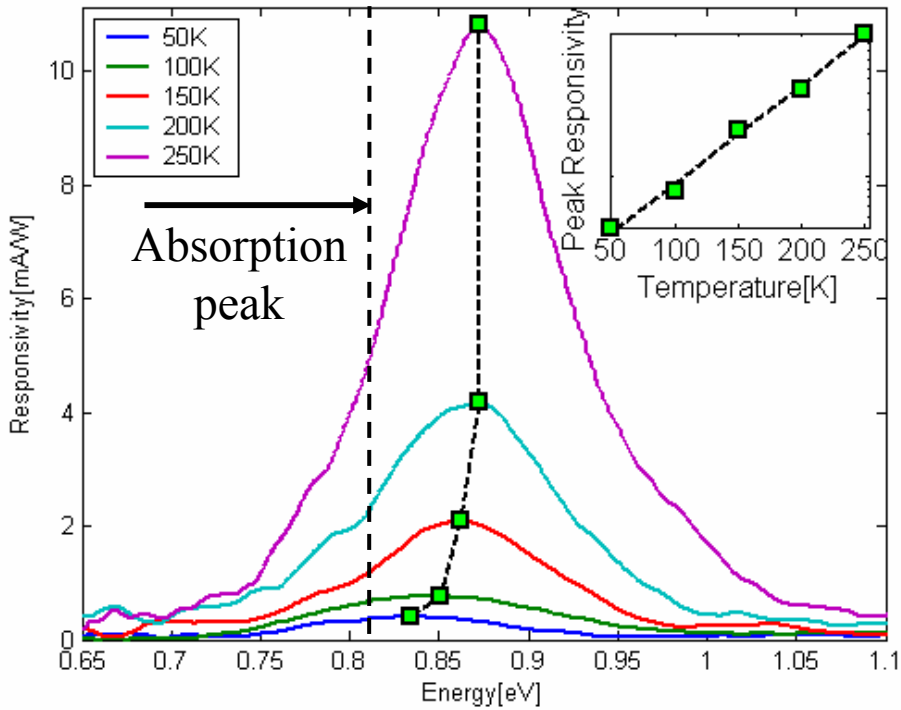

The photocurrent and the blue shift of PC with respect to absorption decrease with temperature lowering

Model assumptions

1. The inhomogeneous broadening of the PL spectra is due to dot size distribution.
2. Dots with Pz above the WLGS can contribute the photocurrent with high efficiency. Dots with Pz below the WLGS can contribute too, but with low efficiency.
3. Fermi level is above the absorption peak but below the WL cutoff.
4. Constant number of electrons in the dots

Lateral Device

1D Eight band K·P model

Pseudomorphic biaxial strain:

$$\in_{xx}, \in_{yy} = \frac{a_{GaN} - a_{AlN}}{a_{AlN}}, \quad \in_{zz} = -2\frac{C_{13}}{C_{33}} \in_{xx}$$

Periodic boundary conditions:

$$E_W = -\frac{\Delta P}{\varepsilon} \cdot \frac{L_B}{L_W + L_B}, \quad E_b = \frac{\Delta P}{\varepsilon} \cdot \frac{L_W}{L_W + L_B}$$

$$\Delta P = P_W - P_B$$

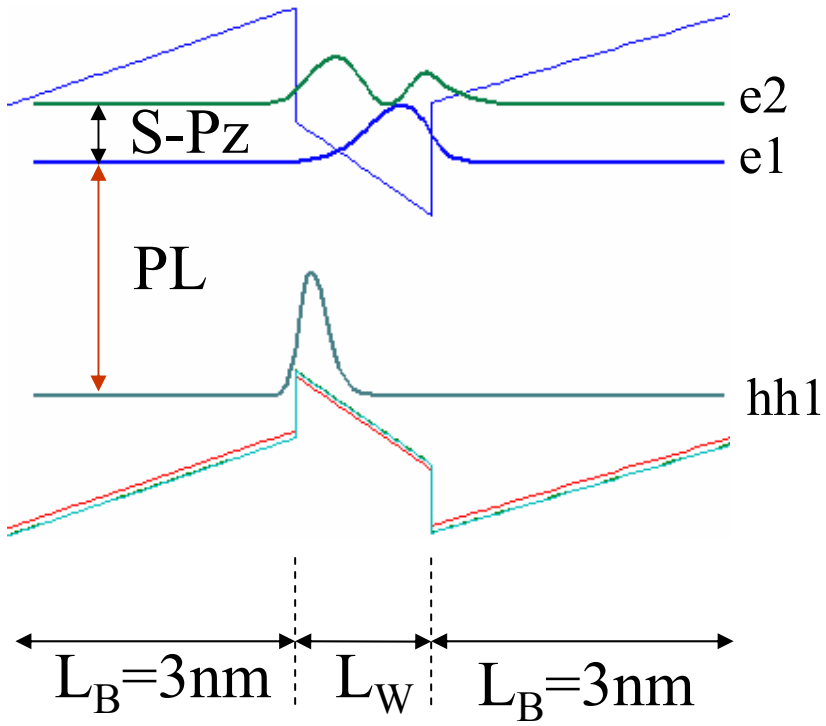

Lateral Device

1D Eight band K·P model

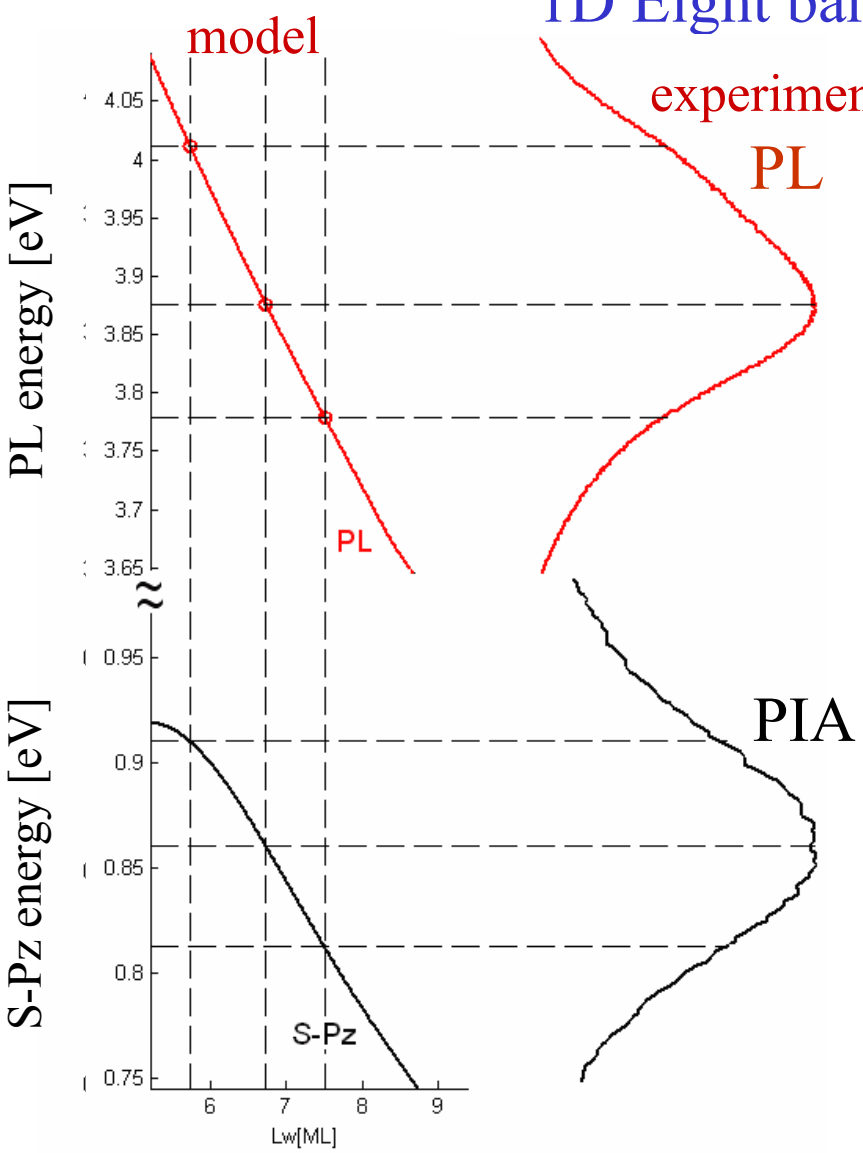

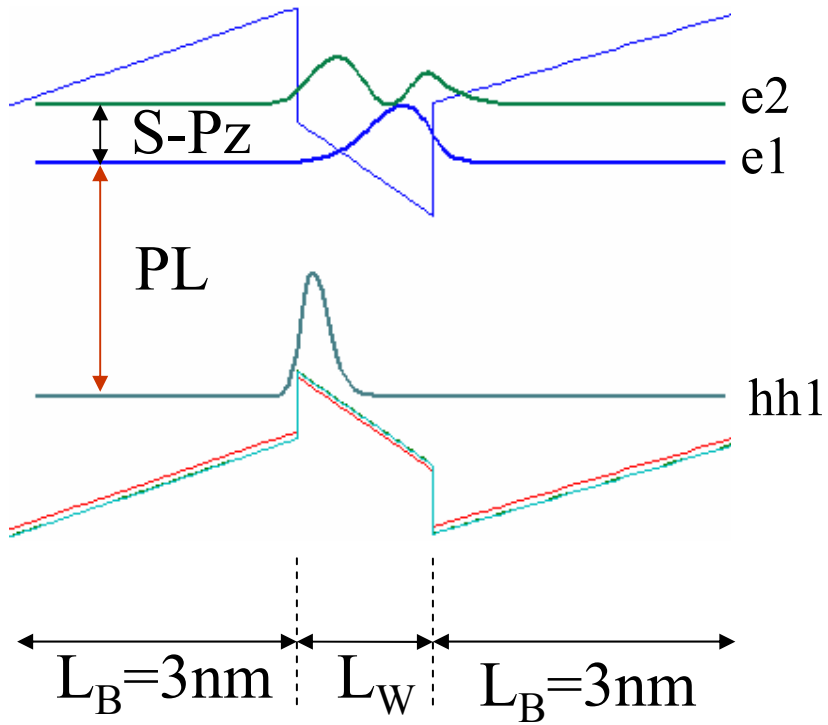

Lateral Device

1D Eight band K·P model calculation

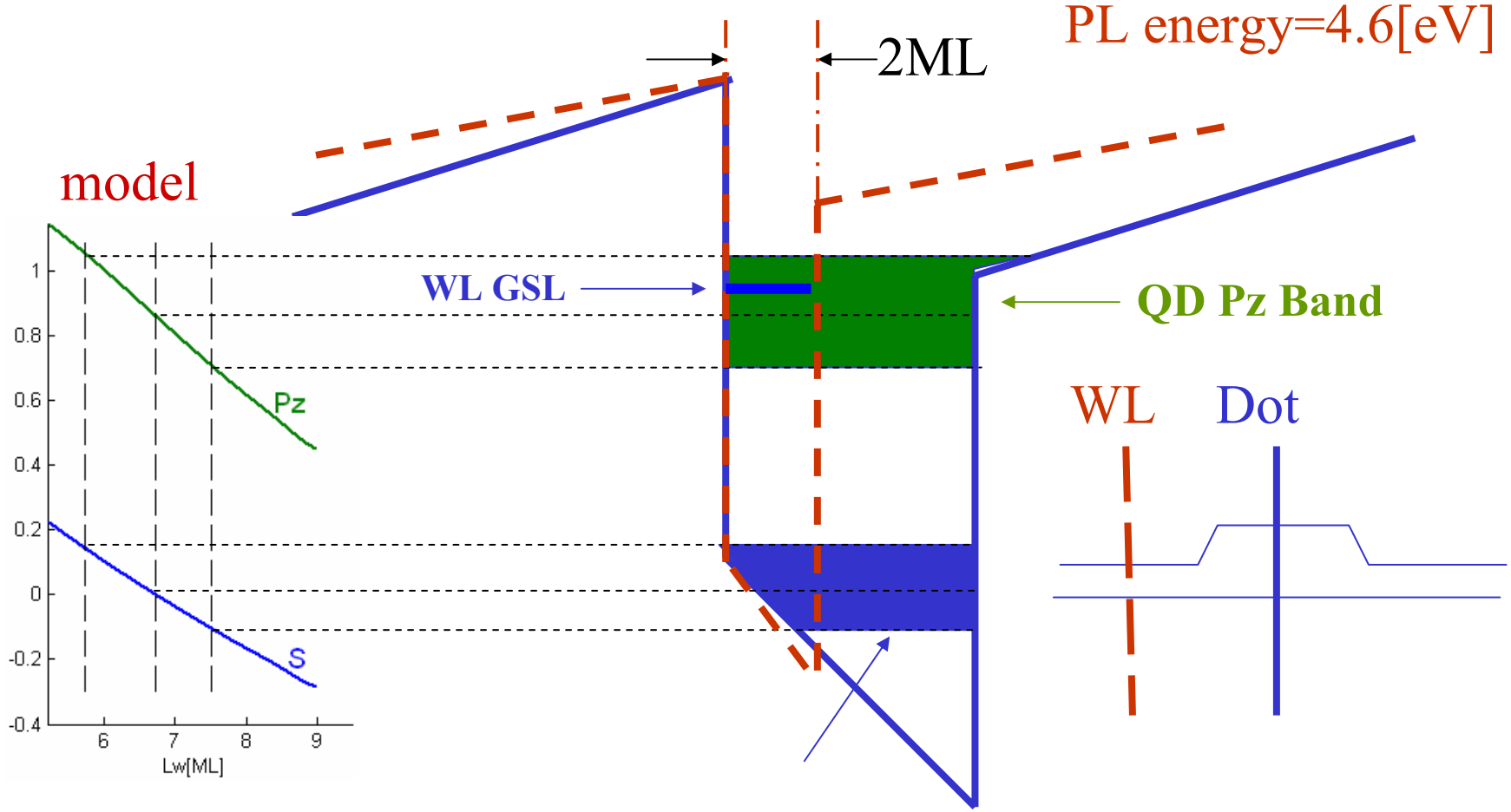

QD S Band width due to fluctuation of $\pm$ one ML

Lateral Device

1D Eight band K·P model

Big Dots

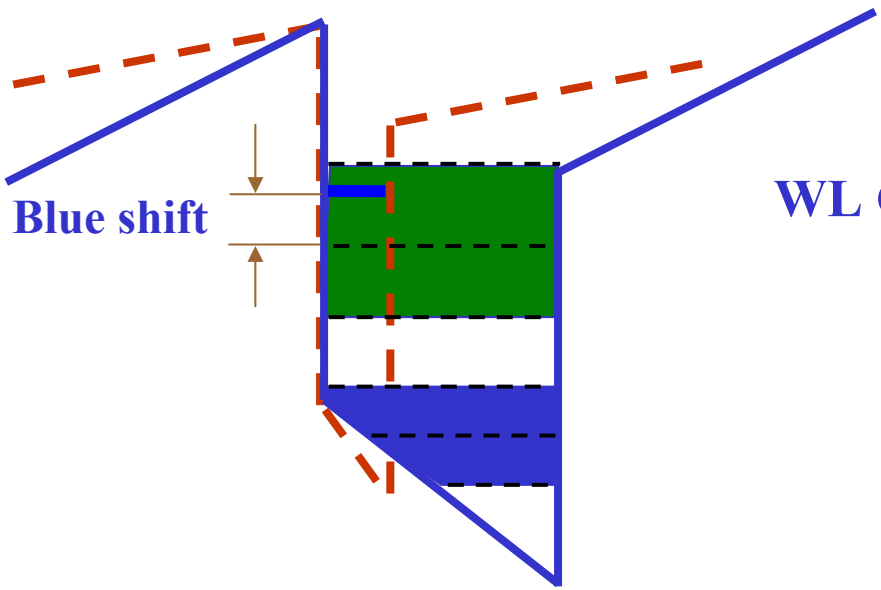

Small Dots

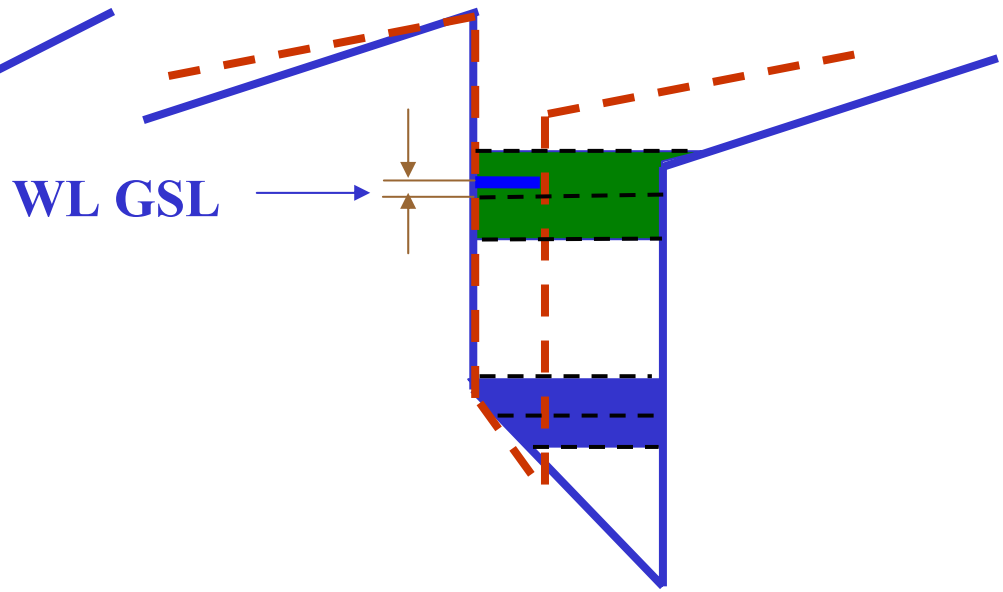

Lateral Device

1D Eight band K·P model

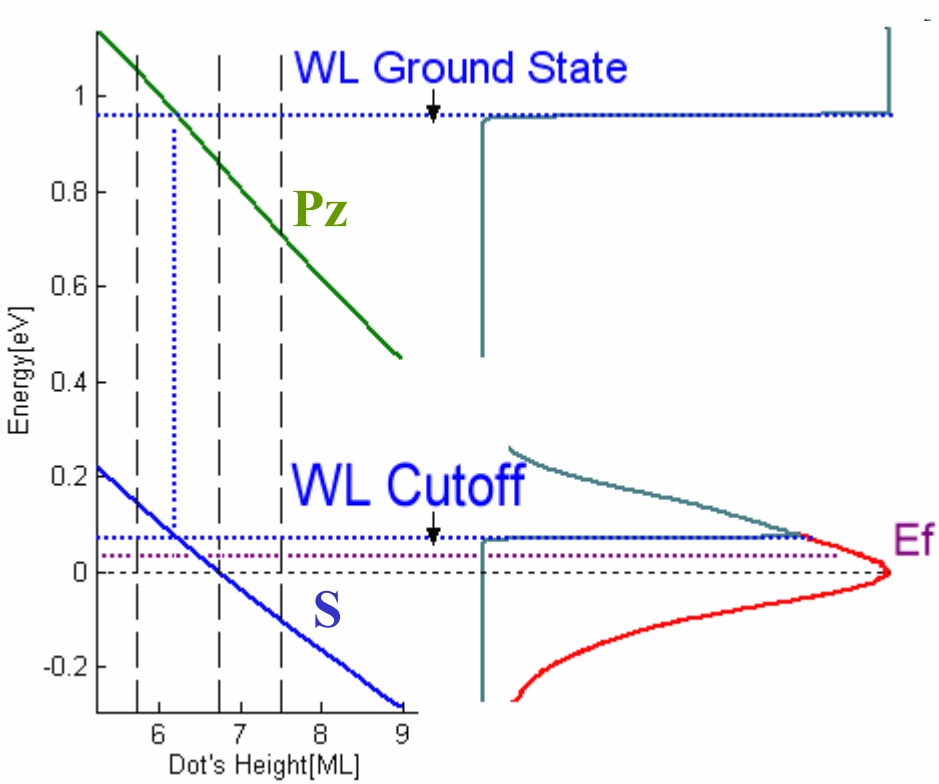

The inhomogeneous broadening of the PL spectra is due to dot size distribution.

Dots with Pz above the WL can contribute the photocurrent with high efficiency. Dots with Pz below the WL can contribute too, but with low efficiency.

Fermi level is above the absorption peak but below the WL cutoff in the S band.

Lateral device PC as function of temperature

1D Eight band K·P model calculation

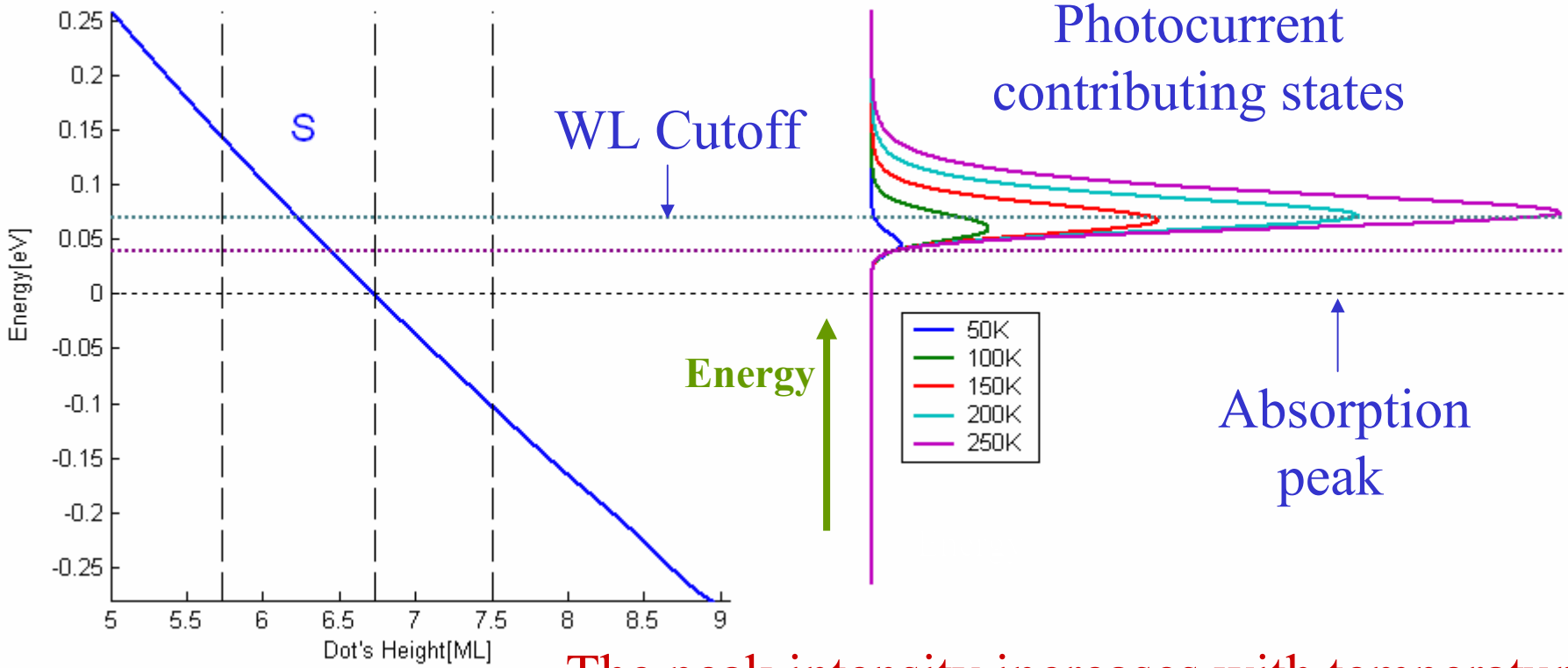

The peak intensity increases with temperature

Peak position decreases with temperature

Lateral Device

Mid IR (MIR) Photocurrent

MIR spectrum can be characterized using photocurrent spectroscopy in normal incident, but in order to characterize the polarization of the transitions, the measurement must be taken in wedge configuration.

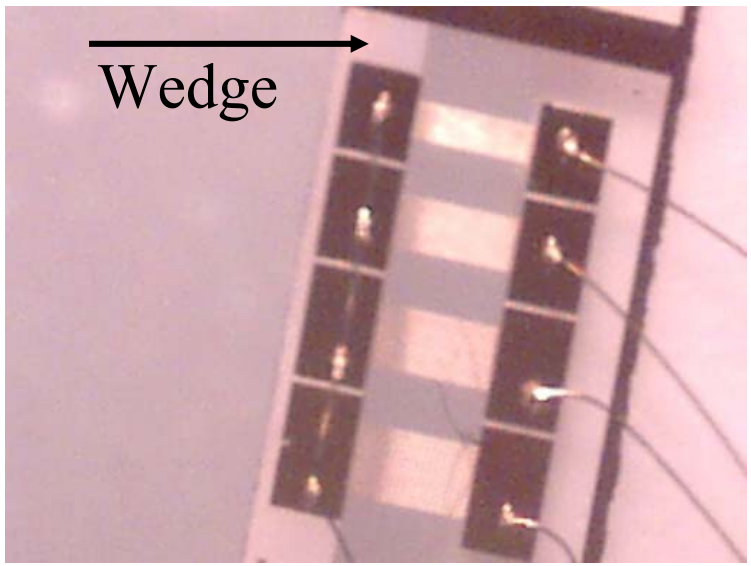

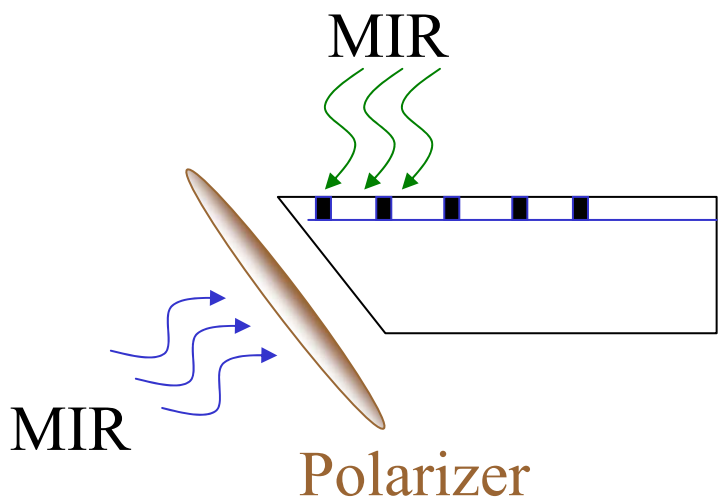

Lateral Device

MIR Photocurrent

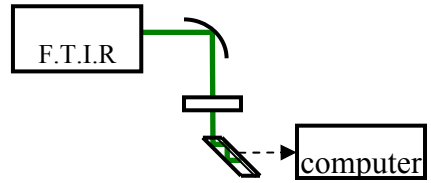

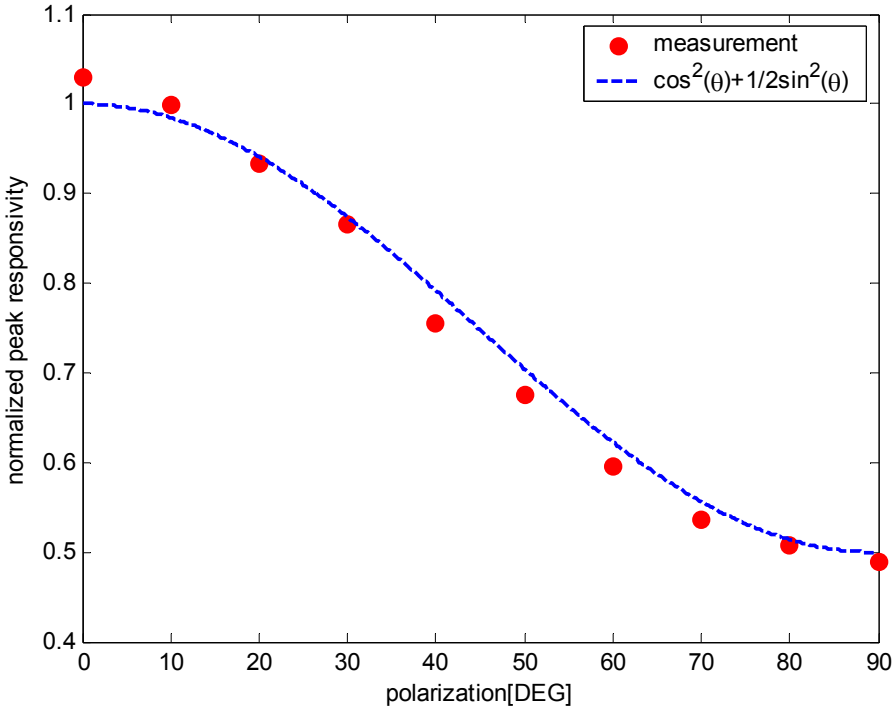

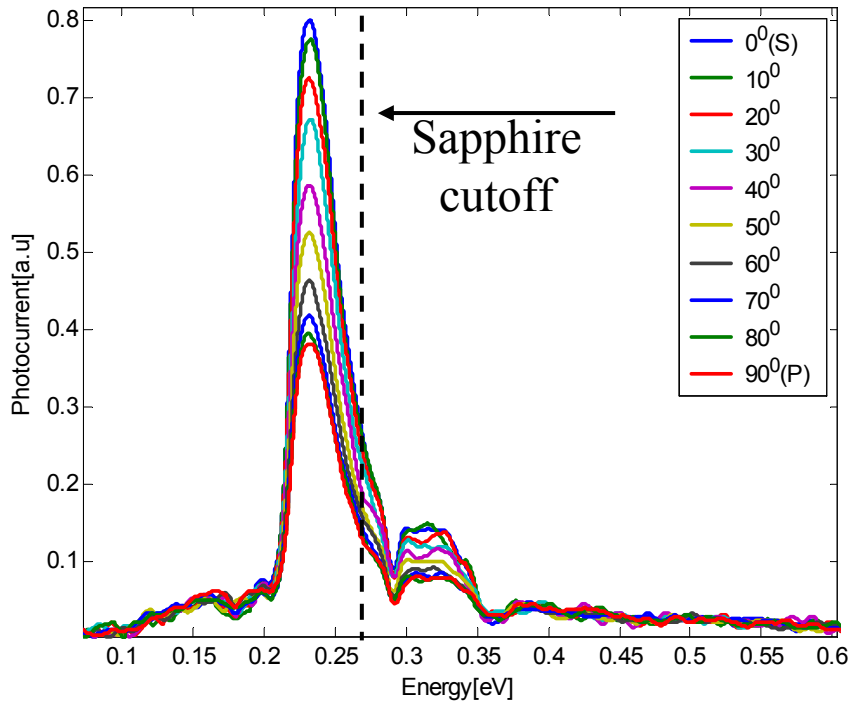

Measured at 12K, using FTIR with glow-bar source.

Lateral Device

MIR Photocurrent

8x8K·P

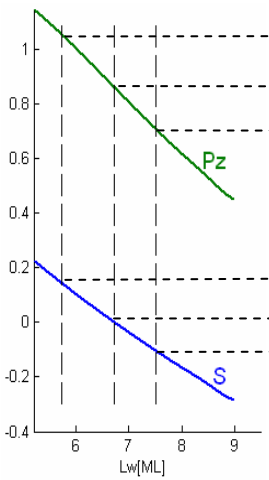

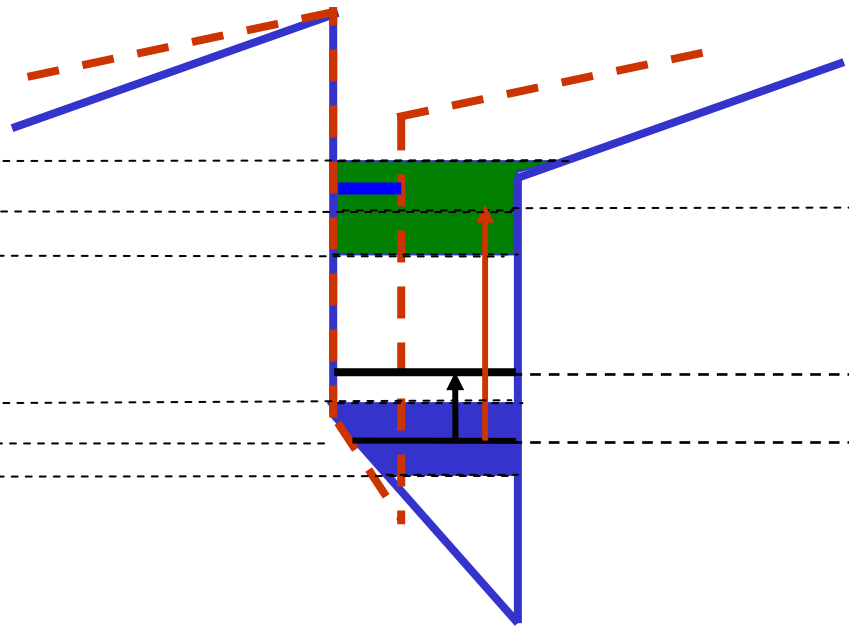

Nextnano

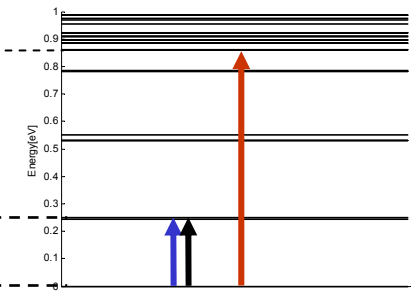

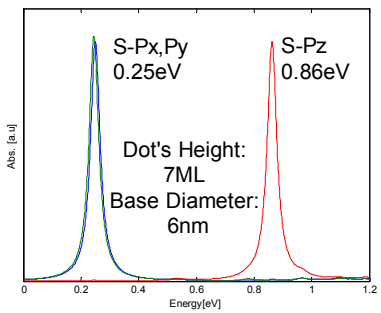

Summary

- Using infrared spectroscopy, we study the conduction band energy levels in GaN\AlN QDs.
- We report on a successful fabrication of telecommunication wavelength photodetector based on intraband transition operating at room temperature.
- A quantitative explanation to the lateral detector photocurrent temperature and dots size dependence was presented.